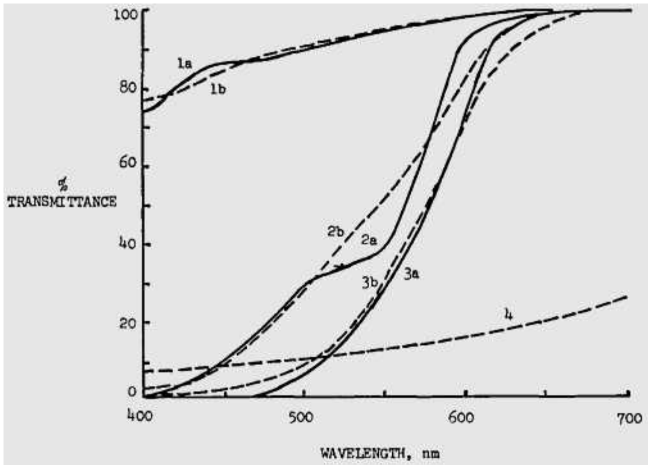

Fig. 3. Transmittance as a function of wavelength for various concentrations of NO_2 and aerosol on a 10-km path with various filters of similar effect.

Curve No.	ppm NO_2	Aerosol Scattering coefficient
1b	0.02	
2b	0.16	
3b	0.4	
4		$2 \times 10^{-4} M^{-1}$ ($\lambda = 550$ nm, $\beta = 3.4$)

	Filter
1a	Wratten 81A
2a	Wratten 86
3a	Wratten 106
4	1.5-mm polyethylene

both aerosol and NO_2 extinction contribute to the final color. The transmitted yellow color of dilute NO_2 can be simulated by a Kodak Wratten 81A filter as shown in Fig. 3, curve 1.

The color of higher concentrations, orange and dark orange, of NO_2 can be simulated by Wratten 86 and 106 filters as shown in Fig. 3, curves 2 and 3. Here, transmission is plotted rather than optical density since the impression of color depends on the light reaching the eye.

Our qualitative, visual observations with these filters suggest that, most of the time in cities, the color effects can be ascribed to wavelength dependent light scattering rather than to absorption by NO_2. On one occasion in the Los Angeles, Calif. area a distinctly yellow color was observed, which might have been due to NO_2, a frequent component of the pollution there. A series of quantitative measurements of the spectral dependence of extinction, made with approximate optical instruments in conjunction with normal pollution monitoring would possibly settle the question of which dominates the color of smog.

References

1. M. Minnaert, The Nature of Colour and Light (Dover Publications, New York, 1954).
2. F. Volz, Thesis, Mainz; Bericht Deutch. Wetterdienstes Nr. 13, Band 2 (1954).
3. N. C. Ahlquist and R. J. Charlson, Atmos. Environ. 3, 551 (1969).

Improved LiF and MgF_2 Overcoated Aluminum Mirrors for Vacuum Ultraviolet Astronomy

M. R. Adriaens and B. Feuerbacher

Surface Physics Division, European Space Research Organization, Noordwijk, Holland.

Received 14 December 1970.

The reflectance of aluminum surfaces overcoated with LiF (Ref. 1) or MgF_2 (Ref. 2) has been measured in the 1050–1600-Å region under ultra-high vacuum conditions and an improved procedure developed for the deposition of protective LiF and MgF_2 covering layers. The stability of such coatings is of importance in developing mirrors for satellite based uv astronomy.

Whilst it is well known that a clean aluminum surface has the highest reflectance in this wavelength region it is essential, in order to avoid oxidation of the aluminum, to deposit a thin protective layer of LiF or MgF_2. Although LiF has its short wavelength cut-off at 1050 Å it is slightly hygroscopic, and the extreme ultraviolet reflectance deteriorates markedly in a normal atmosphere.[2,3] MgF_2 is more stable against the influence of humidity but has its short wavelength cut-off at 1150 Å. Typically, a layer thickness of 150 Å is used in order to optimize reflection for the 1000–1100-Å wavelength region.

By carrying out evaporation in a vacuum of 10^{-10} torr slow evaporation rates for the coating could be used without oxidation, allowing the thickness to be controlled to within 5 Å. The aluminum, of 99.99% purity, was evaporated onto firepolished Pyrex substrates from multistranded tungsten helicoils in an ultra-high vacuum system. The initial pressure was about 2×10^{-10} torr which rose to $\sim 2 \times 10^{-9}$ during evaporation of the aluminum at a rate of 10–20 Å/sec and dropped down again to below 5×10^{-10} torr within 30 sec after completion of the deposition. The thickness of the aluminum film was 700–800 Å, being the thinnest film still opaque in this wavelength region.

The LiF and MgF_2 used for these measurements were high purity crystals made by the Harshaw Company. Both tungsten boats as well as platinum boats were used for evaporation containers with no difference in the final results. The LiF and MgF_2 were outgassed for several minutes and evaporated at a rate of approximately 10 Å/sec at a pressure of $\sim 10^{-9}$ torr. No dependence of evaporation speed on reflectance could be found.

In Figs. 1 and 2 the nearly straight line (1) around 90% represent the initial reflectance of the aluminum mirror.[4] The curves (2) in both figures give the reflectance of the aluminum mirror with a 150-Å thick coating of, respectively, LiF and MgF_2 (Ref. 5). The performance of the overcoated mirror is much less efficient below 1300-Å wavelength than the original aluminum surface. This is due to the fact that the absorption coefficient of evaporated films of LiF or MgF_2 is up to four orders of magnitude larger than that of a bulk crystal.[3,5] The true absorption edge of LiF is located at 1050 Å for a single crystal, but additional absorption processes extend this up to 1350 Å for an evaporated film, giving rise to the drop in reflectance shown in curve (2) of Fig. 1. The reasons for this increased absorption are not known. Etch pit studies to determine dislocation densities in LiF films[6] less than 1000 Å thick did not reveal strain levels more than a factor of 2 above those in the bulk grown samples. Electron microscope examination of replicas of the deposited LiF layers did not show any significant structural defects down to a scale of 200 Å. It was found, however, that the layers could be significantly improved and reflectivities increased at wavelengths shorter than 1300 Å by annealing the deposited films at about 300°C for some 60 h in a vacuum of 10^{-7} torr, using a heater built onto the substrate holder.

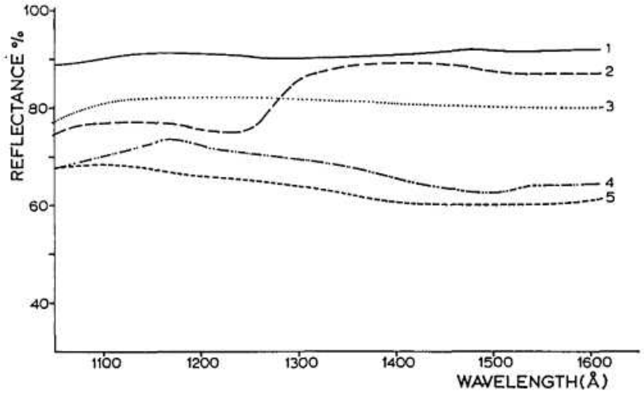

Fig. 1. Overcoating of an aluminum mirror by LiF: 1, initial reflectivity of 700-Å Al on Pyrex substrate; 2, overcoated with 150 Å of LiF; 3, annealed at 300°C for 60 h; 4, aged for 40 days in air; 5. Al mirror with 150 Å, aged for 1 month, from Ref. 7.

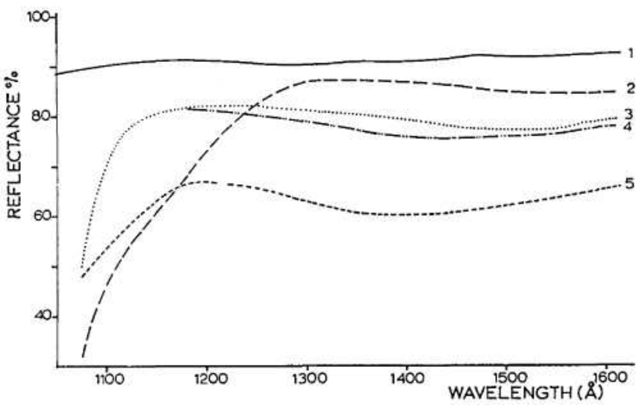

Fig. 2. Overcoating of an aluminum mirror by MgF_2: 1, initial reflectivity of 700-Å Al on Pyrex substrate; 2, overcoated with 150 Å of MgF_2; 3, annealed at 300°C for 60 h; 4, aged 30 days in air; 5, Al mirror with 150-Å MgF_2, not aged, from Ref. 7.

The effect of this annealing on a LiF overcoating is shown in curve (3) of Fig. 1. Although the reflectance in the higher wavelength region is decreased one can see that an improvement of up to 10% is achieved below 1300 Å wavelength.

For a MgF_2 overcoated mirror the effect of annealing is even more marked [Fig. 2 curve (3)]. Here, a maximum improvement of nearly 50% is gained in the wavelength region below 1250 Å, although again there is a slight decrease in reflectance for longer wavelengths. However one of the main advantages of the annealing process is the fact that the annealed mirrors have a far greater resistance to the influence of exposure to the atmosphere. In Fig. 1 [curve (4)] the reflectance is shown of a 150-Å thick LiF overcoated and annealed mirror which had been stored without any precautions in the laboratory atmosphere for 40 days. The humidity of the air ranged between 60–80%. For comparison curve (5) of Fig. 1 shows the reflectance of a mirror overcoated with 140-Å LiF, stored in air for 1 month (humidity 30–50%), this being the best result reported in previous publications.[7]

In case of MgF_2 the effect of storage in humid air is almost negligible as can be seen in Fig. 2, curve (4) which represents the reflectance of a 150-Å thick overcoated and annealed mirror after being stored in air (humidity 60–80%) for 4 weeks. Curve (5) of Fig. 3 illustrates the best result found in previous publications for an aluminum mirror with 150-Å MgF_2 coating but without extended exposure to air.[7]

The results emphasize the usefulness of ultra-high vacuum techniques for making very reproducible highly efficient reflecting surfaces for the vacuum ultraviolet and the application of the annealing process in improving the short wavelength reflectivity and long term stability of the overcoated mirrors.

We thank B. Fitton for his advice and encouragement. We are grateful to R. Willis and M. Barnes for the electron microscope and etch pit studies of these layers.

References

1. G. Hass and R. Tousey, J. Opt. Soc. Amer. **49**, 593 (1959).
2. D. W. Angel, W. R. Hunter, R. Tousey, and G. Hass, J. Opt. Soc. Amer. **51**, 913 (1961).
3. J. T. Cox, G. Hass, and J. E. Waylonis, Appl. Optics **7**, 1535 (1968).
4. B. P. Feuerbacher and W. Steinmann, Optics Commun. **1**, 81 (1969).
5. B. Feuerbacher, B. Fitton, and W. Steinmann, ELDO/ESRO Techn. Rev. **1**, 385 (1969).
6. J. J. Gilman and W. G. Johnston, in Solid State Phys., F. Seitz and D. Turnbull (eds.), (Academic Press, New York, 1962), Vol. 13, p. 147.
7. A. P. Bradford, G. Hass, J. F. Osantowski, and A. R. Toft, Appl. Opt. **8**, 1183 (1969).

Measurement of the Beam Parameters of a Laser

L. M. Vallese

ElectroPhysics Corporation, Nutley, New Jersey 07110.
Received 5 January 1971.

In a recent paper[1] Miyamoto and Yasuura have described an elegant phase method for measuring the beam parameters of a laser, such as beamwidth and radius of curvature of the wavefront, using a hologram. The purpose of the following communication is to show that the same parameters may be obtained more simply by amplitude measurement of the radiant power pattern and comparison with the radiant intensity pattern. However, the phase method would appear to offer greater sensitivity; its technique, not widely used, could probably be extended to other problems.

The field of a spherical-mirror-cavity laser is expressed as[2]:

$$E_{mn}(x,y,z) = A_{mn}\left\{H_m\left[\frac{(2)^{\frac{1}{2}}x}{w_e(z)}\right] H_n\left[\frac{(2)^{\frac{1}{2}}y}{w_e(z)}\right]\right\} \times \exp[-(x^2+y^2)/w_e^2(z)], \quad (1)$$

where the phase angle is not shown, A_{mn} are mode amplitudes, x, y are transverse coordinates, z is the distance from the laser exit aperture to the point of measurement, $w_e(z)$ is the radius at which the amplitude of the fundamental mode decreases to $1/e$ of maximum, H_m is the mth-order Hermite polynomial.

The parameters of interest are the beamwidth $w_e(z)$ and the radius of curvature of the wavefront in the TEM_{oo} mode $R(z) = w_e^2(z)/8z$.

The radiant intensity is proportional to E^2; considering for simplicity the case of the fundamental mode, the intensity is written as:

$$J(x,y,z) = J_o \exp[-2(x^2+y^2)/w_e^2(z)] \quad (2)$$

Converting to spherical coordinates (ρ, θ, ϕ) and assuming small angles and circular cylindrical symmetry, the latter relationship yields